14

Comparison of Energy-Based and Damage-Related Fatigue Life Models for Aluminium Components Under TMF Loading

Eichlseder Wilfried, Winter Gerhard,
Minichmayr Robert and Riedler Martin
Montanuniversität Leoben
Austria

1. Introduction

Thermo-mechanical fatigue is generally due to a cyclic thermal load in conjunction with restrained thermal expansion. Because of the considerable amplitude of strain this load leads to local cyclic plastic deformation and thus to material fatigue. Usually several concurrent and complex damage mechanisms are involved in thermo-mechanical fatigue due to the temperatures and stresses attained. In addition to typical fatigue damage caused by plastic deformation, elevated temperature leads to an increase in corrosive effects (e.g. oxidation) and creep damage. The areas of application are manifold: besides thermo-mechanical fatigue of combustion engine components (e.g. cylinder heads, pistons, exhaust elbows) such effects are common with tanks used in the chemical industry, pipelines, braking systems, turbine blades, as well as all machine tool components and components subjected to elevated operating temperatures. All these applications show cyclic thermal load which, for example, is caused by start-up and shutdown procedures, as well as a mechanical load caused by either restrained thermal expansion (e.g. cylinder heads) or considerable centrifugal forces (e.g. turbine blades).
While in 1992 the maximum specific power for a diesel passenger car was 35 kW/l, the typical ignition pressure was about 130 bar, resulting in a maximum piston temperature of 330 °C. Owing to demands targeting reduction of costs, emissions and fuel consumption, an increase in efficiency by means of "Downsizing" is called for. This is realised by reducing the cubic capacity as well as the number of cylinders and along with additional charging, resulting in an increase in firing pressures and temperature the combustion chamber. The specific power thus obtained is in the region of 70 kW/l, together with ignition pressures of 200 bar and a maximum piston temperature of more than 400 °C, (Reichstein, 2005).
Modern cylinder head materials are typically produced out of aluminium-cast alloys, of which aluminium-silicon-magnesium (AlSiMg) and aluminium-silicon-copper (AlSiCu) alloys are most common. Aluminium and silicon form a eutectic at 577°C and 12 weight percent. The Al-solid solution, silicon and additional secondary phases have a eutectic solidification. The cooling rate influences the dendrite arm spacing (DAS) and the morphology of the eutectic silicon. A high cooling rate leads to a low DAS and finer secondary microstructure. The hypoeutectic alloys are used for cylinder heads and hypereutectic alloys are found in pistons and crankcases.

2. Similarities and differences between LCF and TMF

By their very nature, cyclic thermal loads appear with relatively low numbers of cycles in the low cycle fatigue (LCF) region so that the application of strain-based concepts (e.g. strain life diagrams etc.) is self-evident. If the loading is large enough to produce plastic strain, the number of cycles to failure is relatively low, in the order of less than 10,000 cycles. This total strain predominantly consists of plastic strain, which dominates the fatigue life. Widely used methods to determine the material behaviour are total strain based fatigue tests, whereby the resulting cyclic stress-strain hystereses are investigated. The resulting cyclic stress-strain curves as well as strain S-N curves are the basis for further lifetime evaluation where, depending on the material behaviour, softening or/and hardening effects can be found.

Depending on the application, further influences like temperature, mean strain, strain rate, atmosphere or aging-conditions must be considered. The components are primarily obtained by casting and defects such as pores, shrink holes or oxide inclusions ensued during this process have a negative influence on the lifetime. While these influences are extensively studied for isothermal conditions (Fagschlunger et al., 2006, Oberwinkler et al., 2010, Powazka et al, 2010), scientific understanding of the same for TMF is very limited. While LCF tests are always conducted under isothermal conditions, TMF tests are additionally loaded by thermal cycles, normally defined by a minimum and maximum temperature, dwell time and heating/cooling rates.

As TMF experiments are both very cost-intensive and time-consuming, it is often attempted in practice to estimate the fatigue life of components under thermo-mechanical load by means of more common isothermal LCF experiments. However, this approach may lead to non-conservative fatigue life estimates if the cyclic stress-strain behaviour or the effective damaging mechanisms under TMF loading differ considerably from the material behaviour under isothermal conditions. Furthermore LCF and TMF test results might not correlate due to differing methods used for recording and interpreting the deformation behaviour. In order to avoid misinterpretations it is crucial to pay close attention to the locally and temporally fluctuating temperature field, in particular when recording the TMF deformation behaviour. Thus a fundamental examination of the stress-strain behaviour and the predominant damage mechanisms under TMF conditions is crucial in order to enable accurate fatigue life predictions under thermo-mechanical fatigue loading. This approach can also clarify to which extent the employment of isothermal data is justified (Riedler et al., 2004; Riedler, 2005).

Differences may result from the fact that under TMF loading, as opposed to isothermal LCF loading, during every cycle a broad temperature range is experienced, in which the material properties can change and the material response may differ. The key to a comparison of LCF and TMF data thus lies in the evolution of the microstructure, whose integral behaviour is reflected in the shape of the stress-strain hysteresis loops.

3. Damage mechanisms in thermo-mechanical fatigue

The phenomena during thermo-mechanical fatigue are influenced by a variety of processes within different temperature ranges during a thermal cycle, where especially at elevated temperatures the mentioned damage mechanisms can occur either individually or in mutual interaction. Thus the predominant damage processes are thermally activated gliding of

dislocations at low temperatures, cyclic ageing at medium temperatures, and diffusion creep at high temperatures. However, both under IP (temperature and stress cycle are in phase) and OP (temperature and stress cycle are out of phase) TMF loading the microstructure evolution and the oxidation processes are more often than not dominated by the temperature range close to the maximum temperature. The maximum temperature occurs in the tensile stress region in case of an IP-TMF load, and in the compressive stress region in case of an OP-TMF load, see figure 1 (according to Löhe et al., 2004) and figure 2.
On the other hand concerning OP-TMF, crack initiation and growth are linked directly with the processes in the temperature range closest to the minimum temperature where tensile stresses prevail, and are only linked indirectly with processes that occur at the maximum temperature. Nevertheless this indirect influence can be even more distinctive than it would be in isothermal experiments. For example a layer of scale might build up as a result of oxidation which takes effect predominantly at high temperatures. This layer of scale is very brittle at low temperatures and thus causes early crack initiation and accelerated crack propagation under an OP-TMF load.

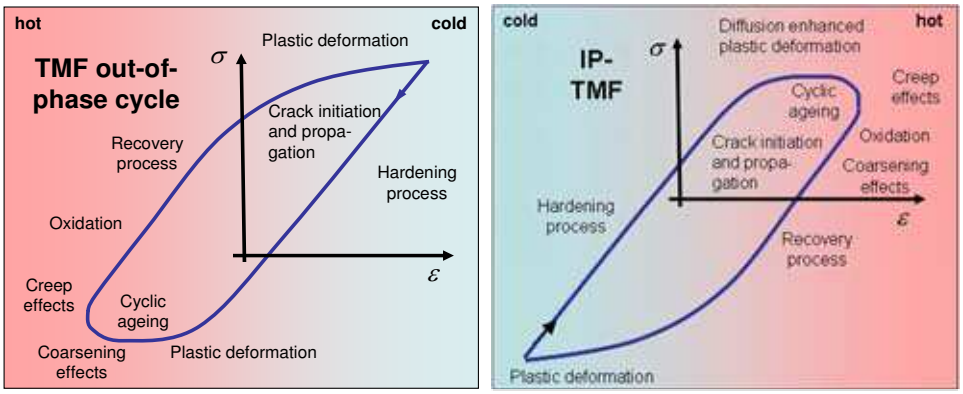

Fig. 1. Active damaging mechanisms during an OP- and IP-TMF cycle (Löhe et al., 2004)

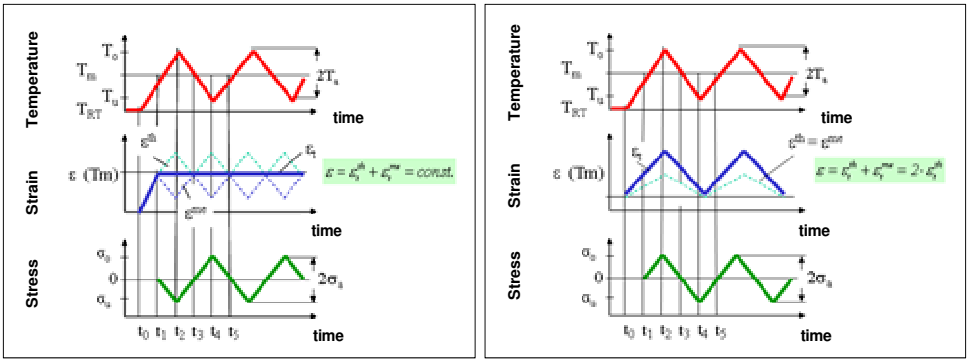

Fig. 2. History of temperature, strain and time under OP-TMF loading (on the left) and IP-TMF loading (on the right)

Crack initiation in various Al-Si-alloys occurs preferentially at the interface between Al-matrix and Si-phase. A meso-scale modelling of the microstructure under thermo-mechanical loading conditions shows stress concentration in the Al-Si-interface (Thalmair, 2009). The repeated recurring thermo-mechanical cycles cause micro-stresses and hence the preferred crack initiation.

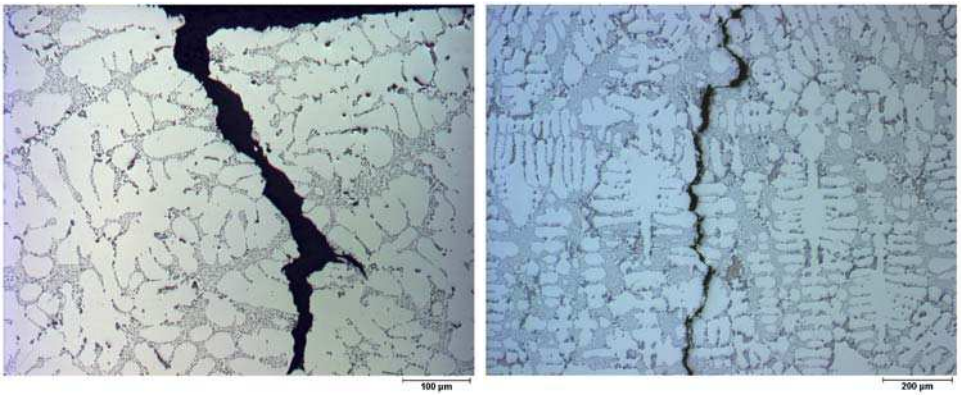

Fig. 3. Crack tip of a TMF-specimen (left) and a thermo-shocked cylinder head (right) of AlSi8Cu3 (Thalmair, 2009)

TMF-test as thermo-shock test of a cylinder head shows very similar crack behaviour, where cracking of the eutectic phase and an inter-dendritic crack-propagation along the interfaces is observed, see figure 3.

4. Methodology

Owing to the multiple effects in components exposed to TMF loading, the developed testing methods are rather varied. Meanwhile, besides LCF experiments and *bi-thermal tests* (Halford et al., 2004) also TMF experiments with combined temperature and strain control are also common. Because of the missing standardisation and the different requirements the experiments differ significantly with respect to heating and cooling temperature application, measurement and control as well as cycle form, strain measurement and consideration of thermal strains. Data from the literature typically allow for little comparability as the information concerning the testing procedures is usually insufficient.

The mechanical loading force application is mostly achieved by means of servo-hydraulic or electro-mechanic testing machines. For this purpose, test equipment manufacturers have started to offer powerful all-in-one systems. However, for special experiments one is still dependent on adaptions or self-made constructions (Riedler & Eichlseder,2004; Minichmayr et al., 2005). Furthermore, it is common to examine specimens with geometries close to the actual component, which only require temperature control. In this case the geometrical constraint is provided for either by the specimen shape or by the mechanical boundary conditions (Simon & Santacreu, 2002; Prillhofer et al., 2005).

It is often tried to simulate the actual behaviour of the component by means of laboratory tests such as for example multiaxial TMF experiments (Otaga & Yamamoto, 2001) or superimposed HCF loading (Minichmayr et al., 2005). By measurement of real components

it is possible to identify actual TMF cycle shapes, which are translated to the test specimen as *industrial cycles* with certain phase shifts between thermal and mechanical strains (Engler-Pinto et al., 1995).
The description of the creep, TMF and LCF testing rigs used for the following experiments as well as a detailed material characterisation can be found in previous papers (Riedler, 2005; Riedler & Eichlseder, 2004; Minichmayr et al., 2005; Minichmayr, 2005).

5. Investigated influences

Firstly, it is important to clarify the governing damage mechanisms that occur in out-of-phase TMF cycles in cylinder heads. Therefore the tests on specimens were specifically designed to take the real circumstances in components as best possible into account – with the aim of using the derived models for lifetime estimations of TMF loaded components. Investigated influences are amongst others (see test matrix in Table 1) mean and local strains, cyclic and constant temperatures, dwell times, pre-aging and aging during service life, HCF-interaction, strain and temperature rates as well as the ratio of mechanical and thermal strain. Further single and multiple step creep tests have been carried out to take into account the stress relaxation phenomena. Additional tests in an argon atmosphere have finally enabled the isolation of the predominating damage mechanism in cylinder heads. All analyses are done in the manner of hysteresis loops, stress-cycle and plastic strain-cycle plots, lifetime diagrams and cyclic deformation behaviour diagrams.

Quasistatic - Creep	LCF	TMF	HCF	Metallographic
Constant temperature	Constant temperature	Maximum temperature	Constant temperature	Fractured surface
Pre-aging	Dwell time	Dwell time	Notch effect	Microstructure
Strain rate	Pre-aging	Pre-aging	Pre-aging	Chem. analysis
Single/multiple step	Mean strain	Mean strain	Dendrite arm spacing	Dendrite arm spacing
Stress relaxation	Strain rate	Temperature rate	Porosity	Porosity
	In lying hole	Rigid clamped - controlled	Mean stress	Precipitations
	Strain amplitude	Strain constraining	Frequency	Grain size
	Argon atmosphere	HCF interaction	Type of loading	Striations
	Incr. step test	Phase shift	Stress amplitude	

Table 1. Test matrix

5.1 Influence of an in lying drilled hole

The aim of this study is to investigate the effects of an in lying drilled hole that is used for an improved quality of the temperature control device, presented in (Riedler & Eichlseder, 2004). The behaviour of the hollow drilled sample is calculated with the finite element method, tested with special LCF test series as well as analyzed by means of fractured surfaces on one wrought and one cast alloy. Whereas the influence on AlCuBiPb is visible, even though, marginally in respect on the lifetime behaviour analyzed with the Manson-Coffin-Basquin (Manson, 1954; Lemaitre & Chaboche, 1985; Basquin, 1910). Approach and the cyclic deformation behaviour analyzed with the Ramberg-Osgood (Ramber & Osgood, 1943) approach, at the Aluminium cast alloy AlSi7MgCu0.5 no difference can be ascertained between the test series of the hollow and solid samples (Riedler & Eichlseder, 2004).

Moreover the analysis by means of fractured surfaces of AlSi7MgCu0.5 of the solid and hollow sample of three LCF strain levels shows assimilable fractured surfaces for each strain level. When decreasing the strain level to lower values, a crack propagation area can be seen beginning at the outside of the specimens. The finite element method shows differences that are of the size of less than one per cent from the maximum axial stress (Minichmayr, 2005).

5.2 Influence of pre-aging

When heat treated aluminium alloys are exposed to elevated or fluctuating higher temperatures in their service life, they show a temperature- and time-dependent aging behaviour which can much decrease the mechanical properties. To investigate these effects on low cycle and thermo-mechanical fatigue, LCF test series at room and higher temperatures, as well as LCF and TMF test series for pre-aged conditions were conducted. Moreover TMF test series with different dwell times at the maximum temperatures were conducted to additionally investigate creep effects.

The first investigation is the separated effect of pre-aging (at an elevated constant temperature) on the deformation and lifetime behaviour by the means of quasi static tests, alternating LCF tests (strain ratio=-1) and temperature-controlled OP-TMF tests (temperature ratio=-1). Figure 4 (left) shows the hysteresis loops for two different total strain levels for non pre-aged and pre-aged specimens at 250°C for 500 hours. At the same LCF strain-level the pre-aged specimens show stress values that are about the half compared to non pre-aged specimens. When investigating the influence of pre-aging on the deformation behaviour by means of tensile tests and LCF tests, at the non pre-aged specimens a high stress hardening tendency can be seen as compared to the tensile test. Pre-aging at 250°C for 500 hours leads to a striking by smaller lifetime in the lower strained LCF region. The deformation behaviour of pre-aged specimens in the manner of stress-cycle or plastic strain-cycle plots shows a nearly straight line without any distinctive hardening or softening, but a markedly higher plastic strain part.

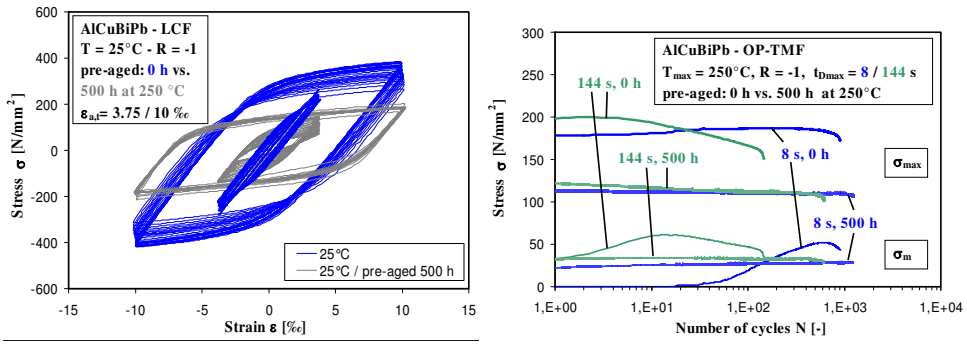

Fig. 4. Influence of pre-aging on the LCF hysteresis loops (on the left) and on the OP-TMF stress-cycle behaviour (on the right)

At the same TMF temperature-level pre-aged specimens at 250°C for 500 hours show the analogous deformation behaviour tendency as obtained at the LCF results, namely a decrease of about 50 per cent compared to non pre-aged specimens, see figure 4 right. The influence of the dwell time decreases with increasing time and temperature of pre-aging.

The differences in lifetime for the dwell time of 8 s and 144 s decreases from a factor more than 6 to a factor of 2, when the specimens are pre-aged for 500 h at 250°C before being tested. After extensive pre-aging the influence of dwell time completely disappears in face of the cyclic deformation and the lifetime behaviour (Riedler & Eichlseder, 2004; Riedler et al., 2005)

5.3 Influence of temperature

A constant elevated temperature influences firstly the quasi static material behaviour and secondly has a time-dependent effect because of hardening vs. softening effects during service life. In this section the time-dependent influence of a constant elevated temperature on LCF is investigated by means of non pre-aged specimens.

A constant elevated temperature of 200°C leads to a higher damage of the material with differences in the lifetime of about one decade compared to the room temperature results. At 250°C the effect is even more drastically, as figure 5 (left) shows. Although at the high strained area the lifetime is a little higher than for 200°C, after the point of intersection at about 100 cycles there is a tremendous drop in the lifetime. Figure 5 (right) shows the summarized presentation of the influences of pre-aging, constant elevated temperature and applied mean strain on the LCF deformation behaviour by means of the plastic strain amplitude part. At a constant temperature of 200°C the stress softening phase starts after a few cycles, what can be seen in an increase of the plastic strain part.

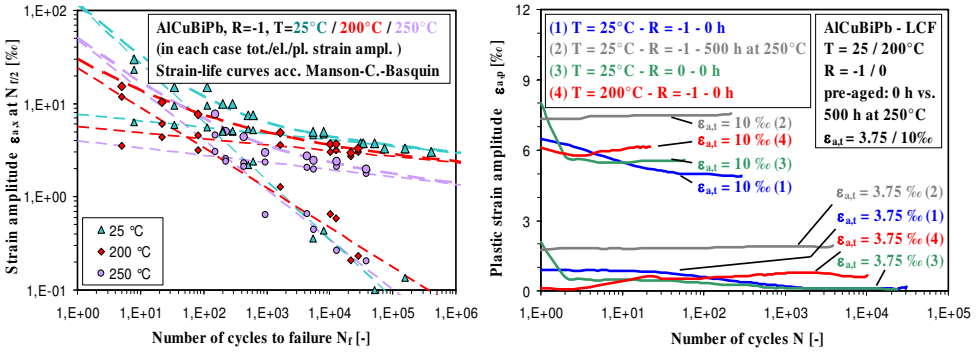

Fig. 5. Influence of elevated temperature on the LCF lifetime (on the left) and influence of pre-aging, elevated temperature and mean strain on the LCF deformation behaviour (on the right)

5.4 Influence of mean strain

Impressed mean strains in the manner of pulsating LCF tests (strain ratio=0) show a visible decrease in lifetime for higher strain levels and only a slight lifetime decreasing effect at lower strain levels. At latest from the half of the number of cycles to failure $N_{f/2}$ on, the cyclic stress deformation curves follow a common progression. Some slight lifetime-decreasing effects ascertainable at pulsating executed test series mostly result from the first few cycles, where the higher tensile stresses and plastic strains (see figure 5 (right)) cause higher damage rates. The comparison of alternating and pulsating executed TMF test series shows the same tendencies as at the LCF results. At latest from $N_{f/2}$ on, the cyclic stress deformation

curves follow a common progression and only some slight lifetime-decreasing effects are ascertainable at pulsating executed TMF test series.

5.5 Influence of dwell-time

The typically start-stop-operation of a motor vehicle as well as the alternating fired and non-fired operation causes dwell times. To study this effect out-of-phase TMF tests with four different dwell times at the particular maximum temperatures were conducted (8, 24, 144 and 864 s).

Whereas with the alloy AlCuBiPb, a higher dwell time always causes a lifetime decreasing effect. This is not the case with the alloy AlSi7MgCu0.5, as figure 6 (left) shows, where the strain values are scaled between the minimum and maximum in this range. The TMF strain-life curve for the dwell time of t_{D3}=144 s is quite steep for higher strain values (and therefore temperatures). A point of intersection of the curves for the lower dwell times (8 s and 24 s) is visible at about 1000 cycles. This phenomenon is explained with pronounced softening effects in the first few cycles that occur due to the high aging tendency at the high dwell time and temperature level. The capacious over-aging at this level can mainly be seen in the highly plastic parts, what results in an upward movement of the total strain-life curve. For that reason the high over-aging at the dwell time of 144 s shows that a high mechanical strain amplitude can be endured for a longer time compared to the smaller dwell times. If the maximum temperatures are low, this effect turns around at the dimensioning level for cylinder heads (about 5000 cycles) and a lifetime decreasing effect is visible with a higher dwell time.

Two extreme LCF tests were conducted at the mean value for the TMF maximum temperatures. A LCF test series at a constant higher temperature of 250°C and one tested at room temperature, but pre-aged at 250°C for 500 hours. Figure 6 (right) shows that these two LCF strain-life curves span the TMF range for all dwell times of the materials investigated, if the mechanical strain (and not the thermal strain) is considered. The comparison of the LCF hysteresis loops at 250°C with comparable mechanically strained TMF hysteresis loops for all dwell times also shows a good accordance. Moreover the cyclic deformation behaviour according to Ramberg-Osgood shows the best accordance of the LCF-250°C curve with the TMF curves. This investigation shows that the macroscopic behaviour is comparable if the aging status is similar (Riedler et al., 2004).

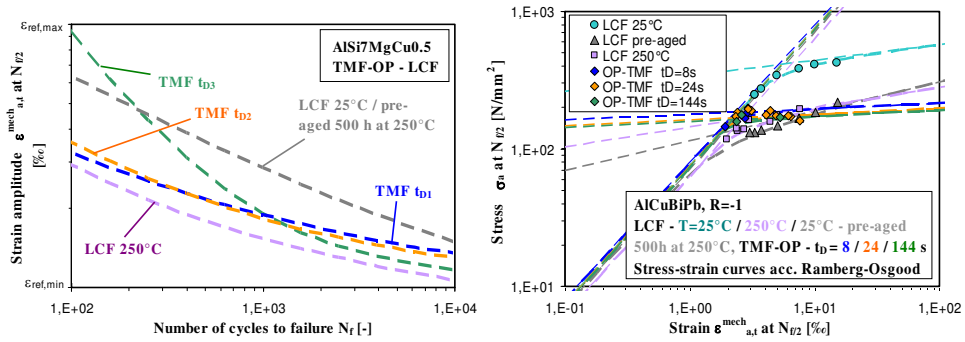

Fig. 6. Influence of TMF dwell-time and LCF-pre-aging and constant elevated temperature on the lifetime (on the left) and on the cyclic deformation behaviour (on the right)

5.6 Influence of phase shifts / strain compensation

In order to investigate the influence of stiffness and phase shifts, different TMF conditions were tested. Besides the ideal OP-TMF situation ($\varepsilon_{t,mech}$=-ε_{th}, K_{TM}=1.0), two overcompensated conditions of the thermal strain (K_{TM}=1.5 and 2.0), a 75% compliance (K_{TM}=0.75, which is near to the real circumstances in cylinder heads) and an ideal in-phase-TMF situation (K_{TM}=-1.0) were tested.

When the local strains are taken into account at rigid clamped specimens, all OP-TMF results can be drawn together in a common strain vs. cycles to failure diagram. Because of creep damage at higher temperatures the IP-TMF lifetime is shorter than the OP-TMF lifetime, as figure 10 shows.

5.7 Influence of strain rates / argon atmosphere

The systematic investigations show that the influence of strain rate on the deformation behaviour is negligible within practical range of temperature rates, but the time and temperature dependent aging behaviour is very important. Unlike the deformation behaviour, the strain rate shows an important influence on the lifetime behaviour due to the additional creep damage involved. These differences and the differences at IP/OP-TMF in the number of cycles to failure allow the separation and investigation of different damage mechanisms. Additional tests in argon atmosphere were executed for this aim, which show a lifetime increasing effect, because of oxidation damage being minimized.

5.8 Influence of HCF interaction

Superimposed HCF-loading has an important influence on the fatigue life of TMF-loaded components. Experiments with superimposed HCF strain amplitudes from 0.01% to 0.1% show a significant decrease in fatigue life depending on the amplitude of the HCF-loads, wherein a small influence of HCF-frequency is found. Metallographic investigations show crack propagation due to HCF-loading and TMF-loading, wherein a combination of HCF-amplitude and the shift in mean-stress causes crack propagation. Good correlation between striations (~crack propagation) and strain amplitude for different loadings is found.

HCF-loadings in a combustion engine occur especially during the heating of the component with maximum ignition pressure. Therefore additional experiments were conducted with superimposed HCF-loadings only during heating period and dwell time. In this case most of the HCF-cycles appear within the compression region of the hysteresis loop. Therefore the effect is obviously reduced. With regard to the typical ignition pressure in a diesel engine, the influence is small compared to the tests without superimposition; see figure 7 (Minichmayr et al., 2005).

5.9 Influence of creep

Because creep effects have to be considered in thermo-mechanical loaded components to take into account stress relaxation phenomena and creep damage, single and multiple step creep tests were carried out. Due to aging effects the decreasing strain rate of the primary creep stage of the single step tests directly merges into the stage of tertiary creep with material softening and therefore increasing creep strain rates. Multiple step tests show, that neither strain nor time are suitable to describe the creep behaviour for that case. Therefore different tests with varying pre-exposure times at test temperature were conducted. The pre-aging time was chosen according to the total time in the multiple step tests. It can be

seen, that the minimum creep strain rate of the single step test at 150 MPa is more than 300 times lower compared to the minimum creep strain rate in multiple step test and single step test with pre-aged specimen at the same stress level. Furthermore the test data of the multiple step test and test with pre-aged specimens show a very similar behaviour. Therefore the time at test temperature determines the minimum strain rate independent of strain (Minichmayr et al., 2005).

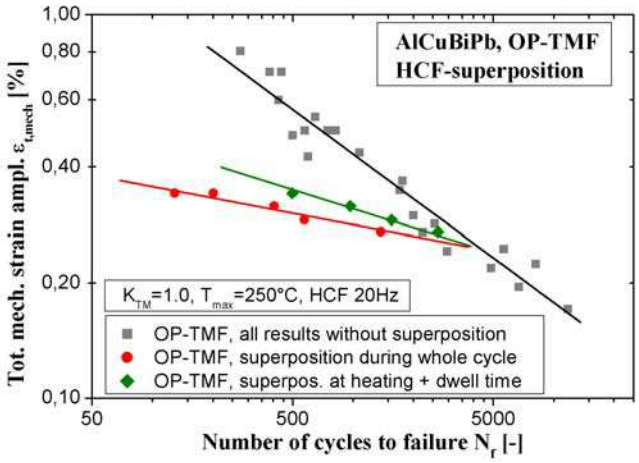

Fig. 7. Influence of HCF interaction on the OP-TMF lifetime

6. Simulation of the cyclic deformation behaviour

6.1 Basics and classification

The description of the elastoplastic deformation behaviour of the construction material forms the basis for assessing the fatigue life of complex components. By means of the finite element method and proper material models it is possible to calculate the local loads (e.g. stress, strain, etc.) under the assumption of adequate boundary conditions.

The most basic material model describes an isotropic plastic hardening independent from the direction of loading. The expansion of the yield surface, which is determined by the *drag stress K* (defined size of the yield surface delimiting the elastic region), can be defined, e.g., in tabular form as a function of the plastic strain. Under cyclic loading each cycle in an isotropic material model leads to further hardening until the maximum strength is obtained and the model shows only elastic, ideal-plastic behaviour. Therefore the isotropic hardening model is adequate only for unidirectional loading. Many materials display the so-called Bauschinger effect under reversed loading (Bauschinger, 1881). The said effect means that plastic deformation occurs already at a significantly lower stress when the load is reversed. The cause of this effect is the formation of dislocation structures, which facilitate plastification in the opposite direction. The Bauschinger effect and the cyclic deformation behaviour, respectively, can only be described by consideration of kinematic hardening, thus using the *back stress* α (which defines the shift of the yield surface in the three-dimensional stress space). In addition high temperatures cause a dependency of stress on the loading rate, which is due to time-dependent processes such as creep. The partitioning

of time-independent plastic deformation and time-dependent creep effects for the deformation behaviour at elevated temperatures is already known from Manson (Manson et al., 1971). At the same time this forms the basis of the *strain range partitioning* concept.
A literature review yields a great number of material models which are able to describe the material behaviour for certain kinds of loading. According to (Christ, 1991) they may be classified according to the underlying approach as follows: empirical models, continuum-mechanical models, physically based models and multi-component models.

6.2 Using the ABAQUS Combinend Hardening Model

The cyclic deformation behaviour is described by the ABAQUS® *Combined Hardening Model* dependent on temperature and ageing. The corresponding variables are the temperature-corrected time and the current temperature. The necessary parameters can be correlated with the $R_{p0,2}$ yield limit from the Shercliff-Ashby model (Shercliff & Ashby, 1990). For the calculation of different states of ageing a user subroutine has been developed. On the one hand it allows for an accumulation of the temperature-corrected time on the basis of the temperature-time curve for separate calculation steps, and on the other hand it is possible to calculate directly the state of ageing for a certain ageing time according to the local maximum temperature.
The calculated hystereses and stress-time curves conform very well to the measured experimental data (fig. 8). Under TMF load both the asymmetry of the stress-strain hystereses and the stress relaxation in the dwell time region are expressed correctly.

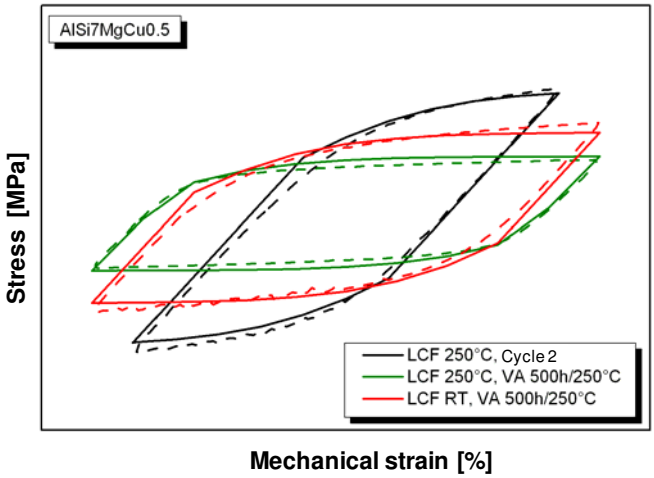

Fig. 8. Comparison of calculated and measured hystereses

7. Simulation of fatigue life behaviour

7.1 Basics and classification

The models available for describing the complex phenomena of thermo-mechanical fatigue range from engineering approaches to physically based models, thereby characterising the combined loading in differing complexity.

Most models for TMF fatigue life calculation are based on linear damage accumulation according to Palmgren-Miner (Palmgren, 1924; Miner, 1945).
Nonlinear cumulative approaches mainly come from Chaboche and Lemaitre (Chaboche & Lesne, 1988; Lemaitre & Chaboche, 1985).
The methods of calculation are mostly based upon local loading parameters such as stress, strain and temperature, which are calculated in complex components by means of elaborate material models. Thus the classification of models describing the fatigue life behaviour under TMF and LCF loading shows the same subdivision as the models describing the cyclic deformation behaviour and shall be briefly explained in the following.

Empirical models

Empirical models represent the major group of this classification. With these models, usually the fatigue life and the parameters of the load cycles are linked. These models are simple, however the partly lacking physical interpretability is a disadvantage.
Furthermore they are effective only for a quite narrow load spectrum as there is no distinction between the individual effects. The empirical models can be set up for various levels of complexity and are divided into approaches based on strain life curves and damage parameters, methods describing creep damage, energy-based approaches, and approaches for partial damage accumulation.

Damage mechanics models

Damage mechanics models usually describe the development of damage by means of methods from continuum mechanics. The origin of these models is found with Kachanov (Kachanov, 1986) and Rabotnov (Rabotnov, 1969) who were concerned with creep damage. Damage mechanics approaches see damage being caused by creep and plastification. As the damage rates are linked to the current damage value, damage accumulation is nonlinear and requires the damage variable to be integrated cycle by cycle.

Physically based models

In general the physically based models play a minor role for practical application, which is due to their complexity and the difficulties in determining their input parameters experimentally. They attempt to characterise the damage development on the basis of atom, vacancy and dislocation movement. At the current state of knowledge and application, physically based models for fatigue life computations are primarily relevant for depicting the physical background of empirical and damage mechanics methods, respectively.

Fracture mechanics models

Fracture mechanics models are linked to the local plastic strains at the crack tip, which can be described, for example, by a ΔJ integral or a modified ΔJ integral, respectively. A link to the physically based models exists with models for micro-crack propagation.

7.2 Application of energetic approaches

An advantage of energy criteria is the significant reduction of parameters in comparison to total strain life curve approaches according to Manson-Coffin-Basquin (Manson, 1954; Coffin, 1954; Basquin, 1910), as energy criteria are able to describe several influences due to the interaction of stress and strain variables. Energy criteria are representative for the cyclic behaviour of materials. They are sound damage indicators which are linked to macroscopic crack initiation and allow for a generalisation to multiaxial loading. The input parameters

have to be known, i.e., the local load parameters in consideration of the cyclic deformation behaviour have to be determined in advance. Especially for aluminium alloys the combination of stress and strain variables yields an adequate parameter as the cyclic deformation behaviour is dominantly affected by the ageing effect. If the temperature dependent ageing reduces the stress, the plastic strain increases in a similar way.
Whilst a single-parameter plastic energy approach is an adequate criterion for the highly ductile aluminium alloy AlCuBiPb, for ductile gravity die casting alloys (AlSi7MgCu0.5 and AlSi8Cu3) it is a total strain based energy criterion. For brittle materials such as AlSi6Cu4 lost foam, a fracture mechanics based energy criterion with a cyclic *J* integral provides the smallest standard deviation (Riedler et al., 2005).
The so-called *unified energy approach* is derived based on this knowledge of material-dependent TMF fatigue life criteria.

$$\Delta W_u = c_u \cdot \Delta W_{u,e} + \Delta W_{u,p} = c_u \left(\sigma_o \cdot \varepsilon_{a,e}\right) + \left(\sigma_a \cdot \varepsilon_{a,p}\right) \tag{1}$$

$$N_B = A_u \cdot \Delta W_u^{-B_u} \tag{2}$$

The specific hysteresis energy for a representative cycle consists of an elastic and a plastic portion. Whereas the elastic portion is formed by the maximum stress and the elastic strain amplitude, the plastic portion is formed by the amplitude values of stress and plastic strain. The material parameter c_u takes values near 1. The fatigue life is determined by a power law approach according to (2). The quality of computing OP-TMF fatigue life for the examined cylinder head alloy made of aluminium and cast iron by means of the *unified energy approach* can be seen in figure 9. It shows 95% of the data points of the six examined alloys influenced by maximum temperature, average and local strain, pre-ageing as well as ageing in operation lying in a fatigue life scatter band of 2.5, and two-thirds of the data points lying in a scatter band of 1.6.

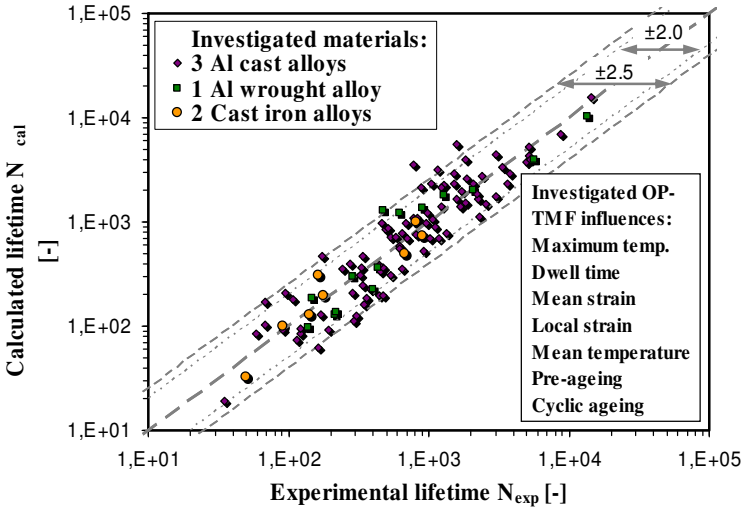

Fig. 9. Quality of the TMF fatigue life simulation by means of the *unified energy approach*

7.3 Application of the damage rate model according to Sehitoglu

The model of Neu-Sehitoglu (Neu & Sehitoglu, 1989) is based on the assumption that overall damage is caused by fatigue, oxidation, and creep:

$$D^{total} = D^{fat} + D^{ox} + D^{creep} \tag{3}$$

or expressed as an equation using the cycles to fracture:

$$\frac{1}{N_B^{total}} = \frac{1}{N_B^{fat}} + \frac{1}{N_B^{ox}} + \frac{1}{N_B^{creep}} \tag{4}$$

The pure fatigue damage portion is described by means of the Manson-Coffin-Basquin approach with the mechanical strain range $\Delta\varepsilon_{mech}$:

$$\frac{\Delta\varepsilon^{mech}}{2} = \frac{\sigma_f^{'}}{E}\left(N_B^{fat}\right)^b + \varepsilon_f^{'}\left(N_B^{fat}\right)^c \tag{5}$$

The parameters E, σ_f', b, ε_f' and c are determined from isothermal fatigue experiments at room temperature. Thereby it is assumed that all experiments at elevated temperature show a similar or shorter fatigue life than at room temperature and furthermore that in these cases the fatigue life reduction is due to the oxidation and creep damage portions.
The oxidation damage portion describes the repeated formation and destruction of an oxide layer at the crack tip as a function of mechanical strain rate, mechanical strain amplitude, temperature and phasing between mechanical strain and temperature:

$$\frac{1}{N_B^{ox}} = \left[\frac{h_{cr}\delta_0}{B\Phi^{ox}K_p^{eff}}\right]^{-\frac{1}{\beta}} \frac{2(\Delta\varepsilon^{mech})^{(2/\beta+1)}}{\dot{\varepsilon}^{1-(\alpha/\beta)}} \tag{6}$$

The temperature dependency of the oxidation is described by means of an Arrhenius approach. The effective oxidation constant is obtained by integration over a complete cycle:

$$K_p^{eff} = \frac{1}{t_C}\int_0^{t_C} D_0 \exp\left(-\frac{Q}{RT(t)}\right)dt \tag{7}$$

The phase factor takes into account that the oxidation damage portion of an OP-TMF load is higher than that of an IP-TMF load:

$$\Phi^{ox} = \frac{1}{t_C}\int_0^{t_C} \phi^{ox}dt \text{ mit } \phi^{ox} = \exp\left[-\frac{1}{2}\left(\frac{(\dot{\varepsilon}^{th}/\dot{\varepsilon}^{mech}+1}{\xi^{ox}}\right)^2\right] \tag{8}$$

The creep damage portion describes the damage due to pore and intergranular crack formation. The creep damage portion is defined as a function of temperature, equivalent stress, hydrostatic stress and *drag stress*:

$$D^{creep} = \Phi^{creep}\int_0^{t_C} A\exp\left(-\frac{\Delta H}{RT(t)}\right)\cdot\left(\frac{\alpha_1\bar{\sigma}+\alpha_2\sigma_H}{K}\right)^m dt \tag{9}$$

It is made use of the internal variables of the material models according to Slavik-Sehitoglu (Slavik & Sehitoglu, 1987). Creep damage is highest under IP-TMF loading, if the maximum temperature coincides with tensile stress. Isothermal LCF experiments show low creep damage, and for OP-TMF loading it is almost zero. Thus another phase factor is introduced:

$$\Phi^{creep} = \frac{1}{t_C}\int_0^{t_C} \phi^{creep} dt \text{ mit } \phi^{creep} = \exp\left[-\frac{1}{2}\left(\frac{(\dot{\varepsilon}^{th} / \dot{\varepsilon}^{mech} - 1}{\xi^{creep}}\right)^2\right] \tag{10}$$

In (Neu & Sehitoglu, 1989) the parameters are determined by means of elaborate experiments. In doing so, also experiments for measuring the oxide layer growth at different temperatures are conducted. Furthermore the growth of the oxide layer under repeated break-up is also measured.
The parameter adjustment in (Minichmayr, 2005)] is carried out solely by manual parameter variation and automatic parameter optimisation. In addition to the OP-TMF experiments (classical cylinder head applications, basis of energetic approaches) also LCF experiments with different strain rates, LCF experiments in argon atmosphere as well as in-phase TMF experiments were necessary. By means of non-linear parameter optimisation the corresponding model parameters were determined.
The fatigue life computation by means of the Sehitoglu damage model is slightly more accurate in comparison to the energy criteria; 90% of the data points for the cast alloy AlSi7MgCu0.5 lie within a scatter band of 1.85. The biggest advantage results from several damage mechanisms being active at the same time. Likewise it is possible, for example, to predict the in-phase TMF experiments correctly, which are characterised by a dominant effect of creep damage, see fig. 10 and 11.

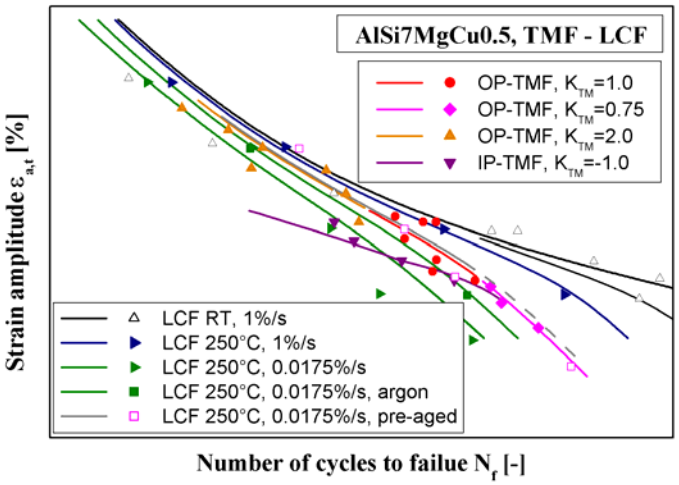

Fig. 10. Fatigue life computing under LCF, OP-TMF, and IP-TMF loading according to the Sehitoglu damage model

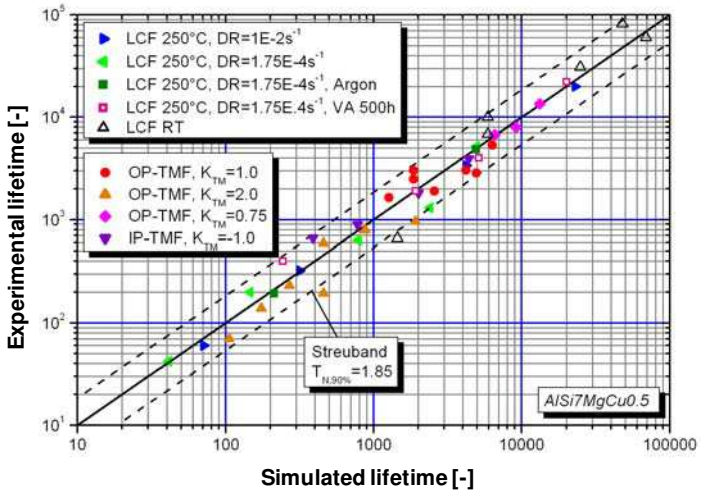

Fig. 11. Quality of the TMF fatigue life calculation using the Sehitoglu damage model

8. Comparative consideration and application to components

Both energy criteria and the model according to Neu-Sehitoglu were used for fatigue life modelling. In contrast to empirical approaches this model distinguishes between different damage mechanisms. The adequate method is chosen according to the type of application; in doing so, it is important to indicate the model limits. Energy criteria seem to represent the best compromise between accuracy and complexity in their application. Major differences occur if the damage mechanisms involved are changing.

Practical application to cylinder heads shows that the fatigue life, calculated on the basis of the dissipated plastic energy, largely depends on the chosen state of ageing. The solution to this problem is an ageing-dependent cumulative damage model.

The commercial fatigue lifetime prediction software FEMFAT (FEMFAT Manual, 2005) features, since version 6.5, a module for calculating the damage under thermo-mechanical loading according to the damage rate model by Neu-Sehitoglu.

With this model it is possible to calculate the local damage portions caused by fatigue, oxidation and creep. The calculation is based on shear strains, which are determined by a critical plane method and are therefore also applicable for multiaxial loading. The predominant part of the overall damage is caused by pure fatigue. The portion of oxidation damage amounts to some 10% in the regions of maximum loading. The fatigue life computation by means of FEMFAT-Sehitoglu provides realistic results concerning the critical areas and fatigue lives.

9. Conclusion

TMF energy criteria is a suitable tool for TMF lifetime assessment of aluminium, provided the limitations of the application are known. They are representative for the cyclic material behaviour and good damage indicators, since they are associated with the macroscopic crack initiation. The damage rate model of Sehitoglu is powerful to describe more influences, albeit with the major disadvantage being the need of an extensive data basis for

every specific material. Depending on the application, one specific lifetime calculation method should be preferred.

10. References

Reichstein, S., Hofmann, L. & Kenningley, S. (2005). Entwicklung von Kolbenwerkstoffen für moderne Hochleistungsdieselmotoren, *Giesserei-Praxis,* pp. 380-384, No. 10, Schiele & Schön, Berlin

Fagschlunger, C., Pötter, K., & Eichlseder, W. (2006). Abschätzung der Schwingfestigkeit von porenfreien Randschichten in Al-Gussbauteilen. *MP Materialprüfung*, pp. 142-151, Vol. 48, No. 4, Hanser, München

Oberwinkler, C., Leitner, H., Eichlseder W., Schönfeld, F. & Schmidt, S. (2010). Schädigungstolerante Auslegung von Aluminium-Druckgusskomponenten, *MP Materials Testing,* pp. 513-519, Vol. 52, No. 7-8, Hanser, München

Powazka, D., Leitner, H., Brune, M., Eichlseder, W. & Oppermann, H. (2010). Fertigungsbedingte Einflüsse auf die Schwingfestigkeit von Al-Gussbauteilen, *Giesserei,* pp. 34-42, Vol. 97, No. 7, Gießerei-Verlag, Düsseldorf

Riedler, M.; Eichlseder, W. & Minichmayr, R. (2004). Relationship between LCF and TMF: Similiarities and Varities, *12th International Conference on Experimental Mechanics*, *ICEM12*, Paper No. 102, Bari

Riedler, M. (2005). TMF von Aluminiumlegierungen – Methodikfindung zur Simulation von thermomechanisch beanspruchten Motorbauteilen aus Aluminiumlegierungen, *Fortschritt-Berichte VDI*, Reihe 5, ISBN 3-18-371805-7

Löhe, D., Beck, T. & Lang, K.-H. (2004). Important aspects of cyclic deformation, damage and lifetime behaviour in thermomechanical fatigue of engineering alloys, pp. 161-175, *Fifth International Conference on Low Cycle Fatigue*, Eds.: Portella, P.D., Sehitoglu, H., Hatanaka, K., DVM, 2004, Berlin

Thalmair, S. (2009). Thermomechanische Ermüdung von Aluminium-Silizium-Gusslegierungen unter ottomotorischen Beanspruchungen, *Dissertation* Univ. Karlsruhe

Halford, G.R., McGaw, M.A.; Bill, R.C. & Fanti, P.D. (1988). Bithermal Fatigue: A Link between Isothermal and Thermomechanical Fatigue, Low Cycle Fatigue pp. 625-637, *ASTM STP 942*, Eds.: Solomon et al., American Society for Testing and Materials, Philadelphia

Riedler, M. & Eichlseder, W. (2004) Temperature control method in elevated and fluctuating temperature fatigue tests, *Materials Engineering*, pp.1-7, Vol. 11, 2004 No. 3, ISSN 1335-0803

Minichmayr, R., Riedler, M. & Eichlseder, W. (2005). Thermomechanische Ermüdung von Aluminiumlegierungen – Versuchstechnik und Methoden der Lebensdaueranalyse, pp. 591-600, *MP Materialprüfung*, Vol. 47, No. 10, Hanser, München

Simon, C. & Santacreu, P.O. (2000). Life Time Prediction of Exhaust Manifolds, pp. 257-267, *Proc. CAMP2002 – High-Temperature Fatigue*, Eds.: Biallas, G., Maier, H.J., Hahn, O., Herrmann, K., Vollertsen, F., Paderborn

Prillhofer, B., Riedler, M. &Eichlseder, W. (2005) Übertragbarkeit von Versuchsergebnissen an Rundproben auf thermomechanisch beanspruchte Bauteile, *1. Leobener Betriebsfestigkeitstage*, Planneralm,

Ogata, T. & Yamamoto, M. (2001). Life Evaluation of IN738LC under Biaxial Thermo-Mechanical Fatigue, pp. 839-847, *Sixth International Conference on Biaxial/Multiaxial Fatigue & Fracture*, Lisboa, Portugal

Engler-Pinto, C.C. Jr., Meyer-Olbersleben, F. & Rézai-Aria, F. (1995). Thermo-Mechanical Fatigue Behaviour of SRR99, Fatigue under Thermal and Mechanical Loading: Mechanisms, pp. 151-157, *Mechanics and Modelling, Kluwer Academic Publishers*, Petten, Eds.: Bressers, J., Rémy, L., Steen, M., Vallés, J.L.

Minichmayr, R. (2005). Modellierung und Simulation des thermomechanischen Ermüdungsverhaltens von Aluminiumbauteilen, Dissertation, Montanuniversität Leoben

Riedler, M. & Eichlseder, W. (2004) Effects of dwell times on thermo-mechanical fatigue, *Zeitschrift Materialprüfung*, Jahrg. 46 11-12, Carl Hanser Verlag, München, S. 577-581.

Bauschinger, J. (1886). Mitt. mech.-techn. Lab., pp. 289, TH München 13, 1886, Zivil-Ing. 27, 1881

Manson, S.S., Halford, G.R. & Hirschberg, M.H. (1971). Creep-Fatigue Analysis by Strain-Range Partitioning, Design for Elevated Temperature Environment, pp. 12-24, Ed.: Zamrik, S.Y., *ASME*, New York

Christ, H.-J. (1991). *Wechselverformung von Metallen*, Springer-Verlag, Berlin

Shercliff, H. R. & Ashby, M. F. (1990). Process Model for Age Hardening of Aluminium Alloys - I. The Model; *Acta metall. Mate*r. Vol. 38, No. 10, 1789-1802, 1990.

Palmgren, A. (1924) Die Lebensdauer von Kugellagern, pp. 339-341 *VDI-Zeitung 58*

Miner, M.A. (1945) Cumulative damage in fatigue, Trans. *ASME Journal of Applied Mechanics*, 12-3, pp. A159-A164.

Chaboche, J.L. & Lesne, P.M. (1988). A Non-Linear Continuous Fatigue Damage Model, pp. 1-17 , *Fat. Fract. Engng. Mater. Struct.*, 11

Lemaitre, J. & Chaboche, J.L. (1985). Mecanique des Materieaux Solides, Dunod,

Kachanov, L.M. On Creep Rupture Time, Izv. Akad. Nauk. SSR, Otd Tekh. Nauk, No. 8, pp. 26-31.

Kachanov, L.M. (1986). Introduction to Continuum Damage Mechanics, Martinus Nijhoff Publ., Dodrecht, Holland

Rabotnov, Y.N. (1969). Creep Problems in Structural Members, North Holland Publishing, Amsterdam

Manson, S.S. (1954). Behaviour of materials under conditions of thermal stress, *NACA Report* No. 1170

Coffin, L.F. (1954). A study of the effects of cyclic thermal stresses on a ductile metal, *Trans. ASME 76*, pp. 931-950.

Basquin, O.H. (1910). The exponential Law of Endurance Tests, *Proceedings of the ASTM 10*, pp. 625-630.

Ramberg, W. & Osgood, W.R. (1943). In: *NACA Technical Note* 902.

Riedler, M., Minichmayr, R. & Eichlseder, W. (2005). Methods for the thermo-mechanical fatigue simulation based on energy criterions, pp. 496-503, *6th International Conference of Assessment of reliability of materials and structures: problems and solutions, RELMAS 2005*, St. Petersburg

Neu, R.W.,6 Sehitoglu, H. (1989). Thermo-mechanical Fatigue, Oxidation and Creep, Part II: Life Prediction, *Metal Transactions*, pp. 1769-1783, Vol. 20A

Slavik, D. & Sehitoglu, H. (1987). A Constitutive Model for High Temperature Loading, Part I and II, in Thermal Stress, *Material Deformation and Thermomechanical Fatigue*, Eds.: Sehitoglu, H., Zamrik, S.Y., ASME PVP 123, New York, 1987, pp. 65-82.

FEMFAT: Finite Elemente Methode und Betriebsfestigkeit, *Manual zur Software FEMFAT*, ECS Steyr, 2005.

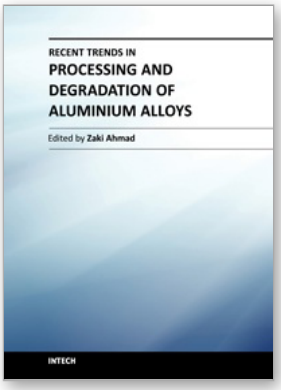

Recent Trends in Processing and Degradation of Aluminium Alloys
Edited by Prof. Zaki Ahmad

ISBN 978-953-307-734-5
Hard cover, 516 pages
Publisher InTech
Published online 21, November, 2011
Published in print edition November, 2011

In the recent decade a quantum leap has been made in production of aluminum alloys and new techniques of casting, forming, welding and surface modification have been evolved to improve the structural integrity of aluminum alloys. This book covers the essential need for the industrial and academic communities for update information. It would also be useful for entrepreneurs technocrats and all those interested in the production and the application of aluminum alloys and strategic structures. It would also help the instructors at senior and graduate level to support their text.

How to reference
In order to correctly reference this scholarly work, feel free to copy and paste the following:

Eichlseder Wilfried, Winter Gerhard, Minichmayr Robert and Riedler Martin (2011). Comparison of Energy-Based and Damage-Related Fatigue Life Models for Aluminium Components Under TMF Loading, Recent Trends in Processing and Degradation of Aluminium Alloys, Prof. Zaki Ahmad (Ed.), ISBN: 978-953-307-734-5, InTech, Available from: http://www.intechopen.com/books/recent-trends-in-processing-and-degradation-of-aluminium-alloys/comparison-of-energy-based-and-damage-related-fatigue-life-models-for-aluminium-components-under-tmf

INTECH
open science | open minds

InTech Europe
University Campus STeP Ri
Slavka Krautzeka 83/A
51000 Rijeka, Croatia
Phone: +385 (51) 770 447
Fax: +385 (51) 686 166
www.intechopen.com

InTech China
Unit 405, Office Block, Hotel Equatorial Shanghai
No.65, Yan An Road (West), Shanghai, 200040, China
中国上海市延安西路65号上海国际贵都大饭店办公楼405单元
Phone: +86-21-62489820
Fax: +86-21-62489821